論文2000-37SD-9-2

캐스케이드된 장주기 광섬유격자 해석에서의 두모드 결합 모델의 유효성

(Validity of the Two-Mode Coupling Model in the Context of Cascaded Long-Period Fiber Gratings)

朴 東 旭*, 黃 俊 皖**
(Dong Wook Park and Joon Hwan Hwnag)

요 약

본 논문에서는 캐스케이드된 장주기 광섬유격자 구조의 해석에 기존의 두모드 결합 모델(TMCM)을 적용할 때에 발생하는 제한요인들에 대하여 분석하고, 아울러 이를 바탕으로 만족 시 TMCM 적용의 유효성을 보장하는 구체적인 조건들을 제안한다. 또한, 실제 상황에서 흔히 찾아 볼 수 있는 격자 파라메터 값을 적용하여 이와 같은 조건들이 의미하는 격자주기 변화의 허용범위와 사용가능 대역폭에 관하여 수치해석 결과를 갖고 논한다.

Abstract

This paper examines the constraints imposed on the usage of the conventional two-mode coupling model in the context of a cascaded long-period fiber grating and presents a set of approximate conditions that must be satisfied for the model to be applicable in the analysis of such a structure. Numerical examples based on the guidelines are provided for a set of realistic grating parameters and their practical implications on the allowed grating period variations for a given bandwidth are discussed.

I. INTRODUCTION

Long-period fiber gratings (LPFG) are currently attracting a great deal of attention, mainly due to their potential in a number of wavelength-division-multiplexing(WDM) applications such as gain flattening and filtering [1-2].

The preferred means of analyzing LPFGs has been the two-mode coupling model (TMCM), which employs the usual coupled-mode theory to describe the grating-assisted interaction between a single core (guided) mode-usually the LP01 mode-and a single cladding mode. In a typical single mode fiber, however, there are a multitude of cladding modes, several of which are capable of interacting with the core mode under right circumstances[3]. As such, one needs to either adopt a rigorous multimode treatment in analyzing the given LPFG, e.g., such as that elaborated in [4], or work within the TMCM's limitation.

Clearly, working with the TMCM is much easier than the alternative, viz., a multimode analysis, but unfortunately, past analyses related to LPFGs have for the most part simply assumed that the TMCM is valid for the given problem without specifically addressing the requirements

* 正會員, ** 學生會員, 弘益大學校 電子工學科
(Dept. of Electronic Engineering, Hongik University)
接受日字:2000年2月28日, 수정완료일:2000年 6月28日

for the model to retain its validity[3]. To that end, we need to explore the issues related to the regime of validity for the TMCM. Specifically, we need to be able to determine: (i) whether the TMCM can be used to analyze the LPFG in a given situation, and (ii) how one should proceed with the design of an LPFG structure within the framework of the TMCM.

This paper is organized as follows. We shall first address the constraints associated with applying the TMCM to a uniform LPFG structure and then generalize the discussion to a composite structure consisting of multiple sections with different grating periods. Based on these discussions, we shall propose a set of approximate rules that can be used in deciding whether the TMCM is applicable to a given problem, which can in turn be used for analysis and design of a LPFG. Some numerical examples of the proposed rules are then presented to illustrate their usage, and the results will be discussed. A brief summary will complete the paper.

Ⅱ. Analysis

Extent of coupling between a core mode and a cladding mode in a long period fiber grating is largely determined by the frequency detuning parameter δ, defined as $\delta \equiv \frac{1}{2}(\beta_{co}-\beta_{cl}-2\pi/\Lambda)$ for a first-order coupling, i. e., coupling via the fundamental Fourier component of the grating's index profile. δ represents the residual discrepancy between the core and the cladding modes' nominal propagation constants β_{co} and β_{cl} after the offset given by the grating's spatial frequency $2\pi/\Lambda$, Λ being the grating's period.

For the TMCM involving a core mode and a particular cladding mode, say the cladding mode p^*, to be valid over a certain spectral region, two requirements must be met simultaneously. One, the normalized detuning parameter $\delta_{p^*}L$ for the cladding mode p^* should be confined within some reasonably small bounds to ensure an adequate coupling with the core mode. Failure to meet this criterion would imply a very weak effect on the propagating waves by the grating, which goes against the purpose of using a grating in the first place. Two, the magnitude of the δ_pL values associated with the other nearby cladding modes should be sufficiently large throughout the wavelength region of concern so that these undesirable cladding modes are essentially uncoupled to the core mode - and thus suppressed - leaving the p^* mode as the only cladding mode of significance worth including in the analysis. Given that the separation between the detuning curves of the p^* mode and the neighboring modes $p' = p^* \pm 1$ in the same section is given by $|\delta_{p^*}-\delta_{p'}| = |\beta_{p^*}-\beta_{p'}|\frac{L}{2}$, it is preferable to select the cladding mode with large differences in the propagation constant (mode index) from its neighboring cladding modes as the main coupling mode p^*. This mode usually turns out to be the fourth or fifth cladding mode in most practical cases. Incidentally, it is assumed in our discussion that the (transverse) coupling coefficients between the core mode and the various cladding modes under consideration are of the same order of magnitude in order to focus solely on the longitudinal aspect of coupling.

Structures consisting of cascaded LPFGs[5] are often employed to obtain the desired spectral characteristics, and they are usually analyzed by applying the transfer matrix method[6]. In the case of cascaded LPFG sections with *different* grating periods, often used for realization of a gain-equalization filter among other applications, issues regarding the validity of the TMCM are further complicated

by the fact that there are a set of δL curves associated with each cladding mode, each curve corresponding to a different grating period (of some constituent grating section). These curves are vertically displaced and also possibly tilted relative to one another because of the variation in the offset term $2\pi/\Lambda$ in the definition of δ and whatever variation that may exist in the lengths of the comprising sections, respectively. Therefore, if the TMCM is to be employed for analysis of a composite structure of this type, all of the δL curves for the desired coupling (cladding) mode p^* must stay confined within a reasonably tight bound *[Condition 1]*. In addition, the δL curves for the other neighboring cladding modes, which are affected by the grating period and section length variations in a similar manner, must remain sufficiently removed from the $\delta L = 0$ axis in all sections to ensure an adequate discrimination against these modes *[Condition 2]*.

Based on the previous discussions, we propose that the following set of approximate conditions must be satisfied in order that the TMCM retain its validity in the analysis of a cascaded LPFG structure. For the sake of generality, let us assume that the cascaded structure consists of N uniform LPFG sections, with the k-th section having length $L^{(k)}$ and grating period $\Lambda^{(k)}$, where the sections are enumerated in the increasing order of Λ ($\Lambda^{(1)} \le \Lambda^{(2)} \le \ldots \le \Lambda^{(N)}$), and that the wavelength region of interest spans $\Delta\lambda$. Furthermore, we assume that $\delta_{p^*}^{(k^*)}$, i. e., the detuning parameter involving the p^* cladding mode in the grating section k^* (with $\Lambda^{(k^*)}$), is zero at the center of the spectral width $\Delta\lambda$. We must then have

$$\mathrm{Max}\{\,|\,\delta_{p^*}^{(k)}L^{(k)}\,|\,\} = \mathrm{Max}\left\{\left|\frac{\beta_{co}-\beta_{p^*}-2\pi/\Lambda^{(k)}}{2}\right|L^{(k)}\right\} \le \phi_1 \quad (1)$$

and

$$\mathrm{Min}\{\,|\,\delta_{p^*\pm1}^{(k)}L^{(k)}\,|\,\} = \mathrm{Min}\left\{\left|\frac{\beta_{co}-\beta_{p^*\pm1}-2\pi/\Lambda^{(k)}}{2}\right|L^{(k)}\right\} \ge \phi \quad (2)$$

where the maximum for the p^* cladding mode in (1), and the minimum for its closest neighboring modes $p^*\pm1$ in (2) are taken over all wavelengths within $\Delta\lambda$ and all grating sections, i. e., over all λ and k values. (1) and (2) correspond to the *Conditions 1 and 2* stated above and require that the normalized detuning parameter values be bounded by some prescribed limits ϕ_1 and ϕ_2, e. g., 2π and 10π, respectively. Only the cladding modes $p^*\pm1$ appear explicitly in (2) - instead of all modes - since their δL curves are located closest to those of the p^* mode.

For the general case in which both L and Λ vary from one section to the next, the expressions above cannot be arranged in a form amenable for easy determination of the constraints on the Λ values. For the special case of all sections having the same length, i. e., $L_1 = L_2 = \ldots = L$, however, inequalities (1) and (2) can be rewritten in the following manner:

$$\mathrm{Max}\left\{\left|\frac{\beta_{co}-\beta_{p^*}-2\pi/\Lambda^{(N)}}{2}\right|_{\lambda_1}, \left|\frac{\beta_{co}-\beta_{p^*}-2\pi/\Lambda^{(1)}}{2}\right|_{\lambda_N}\right\}L \le \phi_1 \quad (3)$$

and

$$\mathrm{Min}\left\{\left|\frac{\beta_{co}-\beta_{p^*-1}-2\pi/\Lambda^{(N)}}{2}\right|_{\lambda_1}, \left|\frac{\beta_{co}-\beta_{p^*+1}-2\pi/\Lambda^{(1)}}{2}\right|_{\lambda_N}\right\}L \ge \phi_2 \quad (4)$$

These expressions can be better understood with the help of Figs. 1(a) and 1(b). In Fig 1(a), the two points marked A and B correspond to the values inside the curly bracket on the LHS of (3) and represent the largest $|\delta_{p^*}L|$ values that occur within the specified bandwidth $\Delta\lambda$. These points are required to be inside the region indicated by the

dashed horizontal lines $\delta L = +\phi_1$ according to the *Condition 1*. Fig. 1(b), on the other hand, shows those δL curves for the adjacent $p^* \pm 1$ cladding modes which are located closest to the $\delta L = 0$ axis. The two points A' and B' with the smallest $|\delta_{p^* \pm 1} L|$ values within $\Delta\lambda$ on those curves are supposed to lie outside the region marked by the horizontal lines $\delta L = \pm\phi_2$ according to the *Condition 2*. In the figures, $\lambda_L = \lambda^* - \Delta\lambda/2$ and $\lambda_R = \lambda^* + \Delta\lambda/2$ are the wavelengths at the left and right edges of the specified bandwidth, located symmetrically with respect to the center wavelength λ^*.

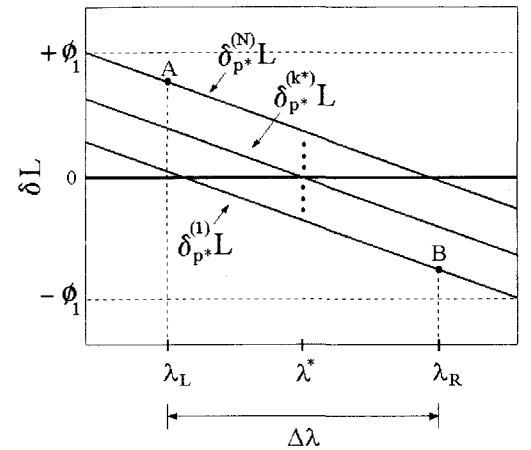

(a)

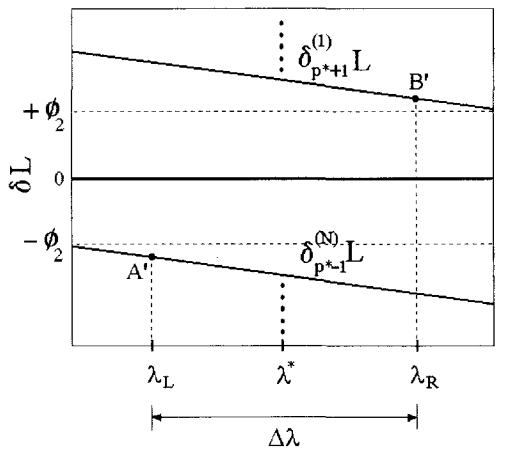

(b)

그림 1. (a) 주어진 상한 위상 값 ϕ_1과 대역폭 $\Delta\lambda$, 그리고 조건 1에 근거한 최대허용 격자주기 변화 $\Delta\Lambda_1$을 찾는 과정의 도식적 설명. (b) 주어진 하한 위상 값 ϕ_2와 대역폭 $\Delta\lambda$, 그리고 조건 2에 근거한 최대허용 격자주기 변화 $\Delta\Lambda_2$를 찾는 과정의 도식적 설명

Fig. 1. (a) Illustration of how the upper bound ϕ_1 may be used to determine $\Delta\Lambda_1$ associated with *Condition 1* for a given $\Delta\lambda$. (b) Illustration of how the lower bound ϕ_2 may be used to determine $\Delta\Lambda_2$ associated with *Condition 2* for a given $\Delta\lambda$.

Based on the above discussions, the upper bound on the grating period variation $\Delta\Lambda$ allowed for a given $\Delta\lambda$ and ϕ_1, ϕ_2 values can be determined as follows. First, we find $\Delta\Lambda_1$, the upper bound on the grating period variation imposed by the *Condition 1* (Eq. (3)), by letting the value of $\Lambda^{(N)}$ increase and the value of $\Lambda^{(1)}$ decrease until the δL values of the two points A and B in Fig. 1(a) are equal to $+\phi_1$ and $-\phi_1$, respectively. $\Delta\Lambda_1$ is given by the difference $\Lambda^{(N)} - \Lambda^{(1)}$ at this juncture. In a similar manner, $\Delta\Lambda_2$, the upper bound on the grating period variation imposed by the *Condition 2* (Eq. (4)), is given by the difference $\Lambda^{(N)} - \Lambda^{(1)}$where $\Lambda^{(N)}$ and $\Lambda^{(1)}$ correspond to the grating periods at which the δL values at the two points A′ and B′ in Fig. 1(b) become equal to $-\phi_2$ and $+\phi_2$, respectively. The overall constraint reflecting both *Conditions 1 and 2* is then given by the lesser of $\Delta\Lambda_1$ and $\Delta\Lambda_2$,values.

For a sufficiently narrow bandwidth $\Delta\lambda$ and a small fractional variation $\Delta\Lambda/\Lambda$ in the grating period, we can obtain approximate expressions for $\Delta\Lambda_1$ and $\Delta\Lambda_2$ (assuming once again all the grating sections have the same length L). Upon approximating the $\delta_{p^*} L$, $\delta_{p^* \pm 1} L$ curves within $\Delta\lambda$ as straight lines, which is reasonable (see Fig. 2 in the following section for an evidence of this), and noting that the slopes $\frac{d\delta_{p^*}^{(k)}}{d\lambda}$, $\frac{d\delta_{p^* \pm 1}^{(k)}}{d\lambda}$, being independent of $\Lambda^{(k)}$, are

same in all sections, we can derive the following results:

$$\Delta\Lambda_1 \approx \frac{2\Lambda^2}{\pi}\left[\frac{\phi_1}{L} - \left|\frac{d\delta_{p^*}}{d\lambda}\right|_{\lambda^*}\frac{\Delta\lambda}{2}\right] \quad (5)$$

$$\Delta\Lambda_2 = \Lambda_U^{(N)} - \Lambda_L^{(1)} \quad (6)$$

where

$$\Lambda_L^{(1)} \approx \frac{\pi}{\frac{1}{2}(\beta_{co}-\beta_{p^*+1})_{\lambda^*} - \left|\frac{d\delta_{p^*+1}}{d\lambda}\right|_{\lambda^*}\frac{\Delta\lambda}{2} - \frac{\phi_2}{L}}$$

$$\Lambda_U^{(N)} \approx \frac{\pi}{\frac{1}{2}(\beta_{co}-\beta_{p^*-1})_{\lambda^*} + \left|\frac{d\delta_{p^*-1}}{d\lambda}\right|_{\lambda^*}\frac{\Delta\lambda}{2} + \frac{\phi_2}{L}}$$

In (5), Λ denotes $\Lambda^{(k^*)}$, the grating period in the k^*-th section wherein the p^* cladding mode enjoys the tightest coupling with the core mode. Although these approximations fail for larger bandwidth values due to the fact that the $\delta_{p^*}L$, $\delta_{p^*\pm1}L$ are not truly linear and have different slopes from one another, they do provide a convenient means of computing the bounds for narrowband applications. Of course, $\Lambda_L^{(1)}$, the lower of limit of $\Lambda^{(1)}$, and $\Lambda_U^{(N)}$, the upper limit of $\Lambda^{(N)}$, in (6) must satisfy the inequality $\Lambda_L^{(1)} \le \Lambda^{(k^*)} = \Lambda \le \Lambda_U^{(N)}$ in order to be consistent with our original assumption $\Lambda^{(1)} \le \Lambda^{(2)} \le \ldots \le \Lambda^{(N)}$.

In this section, we derived expressions for a set of conditions that must be satisfied for the TMCM to be valid. From a practical standpoint, not only do these conditions provide a guideline on the applicability of the TMCM, but they also give us bounds on the usable bandwidth and the allowable grating period differences, *regardless* of how the LPFG device is analyzed. Outside these bounds, the grating's coupling action is very weak and/or several cladding modes are simultaneously coupled with the core mode, degrading the grating device's spectral performance. Specifically, these conditions place a limit on how large a grating period variation can be accommodated in designing a multisection LPFG for a given operating bandwidth, or conversely, how large an operating bandwidth such a device can have for a given grating period difference. Hence, there is a fundamental tradeoff between the operating bandwidth and the allowed maximum grating variation in a composite LPFG structure with different grating periods. Of course, the *bounds* on the bandwidth and the grating period's variation may vary depending on where the bandwidth $\Delta\lambda$ is located, e. g., in the 1.3 μm region or the 1.55 μm region, because the slopes of the detuning curves are wavelength-dependent.

Ⅲ. Numerical Results and Discussion

In this section, we shall present numerical results that serve to illustrate some of the issues raised in the previous section, along with a discussion on their implications. For the computations throughout this section, the grating was assumed to be formed on a standard single-mode fiber, with the core diameter of 9 μm and the cladding diameter of 125 μm. The nominal index figures were assumed to be in the range of 1.4489 - 1.4498 for the core and 1.4439 - 1.4448 for the cladding, after taking the material dispersion into account.

As a first example, consider Fig. 2, in which the δ_4, δ_5 and δ_6 curves *in solid lines* represent the frequency detuning involving the fourth, fifth and the sixth cladding modes, respectively, and the LP01 mode for a particular grating period Λ. We note that because the wavelength region displayed is sufficiently narrow, the δ curves vary with wavelength in a nearly linear fashion, the primary contributor to the variation being the waveguide dispersion. In this particular case, a rather ideal situation

prevails from the standpoint of the TMCM: over much of the spectral range centered at 1.55 μm wavelength, the magnitude of δ_5 maintains a small value whereas those of δ_4 and δ_6 are quite large, implying a tight coupling for the fifth cladding mode and an excellent discrimination against the fourth and the sixth cladding modes. As a figure of reference, $\delta_5 = 100\ m^{-1}$ corresponds to a $\delta_5 L$ value of 2.5 rad for a 25 mm-long grating section, and a difference of $1000\ m^{-1}$ between δ_5 and δ_4 or δ_5 and δ_6 translates to a discrimination of $\Delta(\delta L) = 25$ rad for the same grating length.

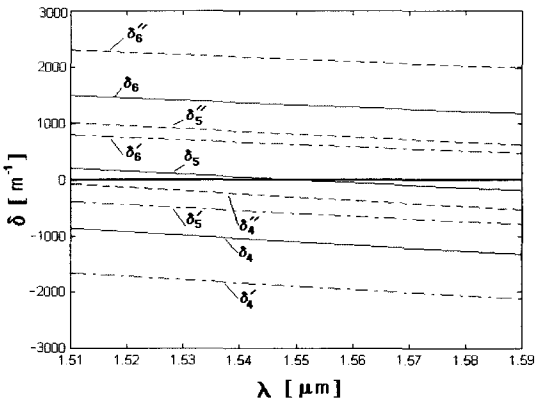

그림 2. 여러 클래딩 모드와 격자주기의 조합에 해당하는 주파수 디튜닝 곡선들

Fig. 2. Frequency detuning curves for several combinations of cladding modes and grating periods.

There are two additional sets of δ curves for the three cladding modes in Fig. 2, each set corresponding to a different grating period: the dash-dot lines denoted by δ' correspond to a shorter grating period (Λ' of Fig. 3 for example) whereas the dotted lines denoted by δ'' correspond to a longer grating period (Λ'' of Fig. 3 for example). Likes of these two sets, along with the set in solid lines, can occur in a composite structure such as the one shown in Fig. 3, which consists of three uniform LPFG sections, each with a different grating period. Note that in the section with the grating period Λ'', the fourth cladding mode now enjoys a better coupling than the fifth cladding mode as evidenced by the relative proximity of the δ_4'' curve to the $\delta = 0$ line. In the section with the grating period Λ', no one cladding mode experiences particularly a tight coupling with the core mode, with both the fifth and the sixth cladding modes having a fairly large detuning parameter value. Because any one particular cladding mode cannot maintain a strong coupling over all three sections, we conclude that the composite structure corresponding to these three sets of δ curves cannot be properly analyzed by the TMCM.

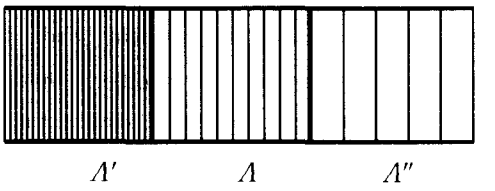

그림 3. 각 구간이 서로 다른 격자주기를 갖고 있는 3-섹션 장주기 광섬유격자 구조의 개략도

Fig. 3. Schematic of a cascaded three-section LPFG structure with each section having a different grating period.

Next, we present a numerical result displaying the relationship between the bandwidth $\Delta\lambda$ and the maximum allowable difference in the grating period $\Delta\Lambda$, based on the two *Conditions* outlined in the previous section. Fig. 4 shows the separate constraints due to the *Conditions 1 and 2,* for a three-section LPFG similar to that of Fig. 3, over the range of $0 \le \Delta\lambda \le 80\ nm$, the upper range being roughly equivalent to the aggregate bandwidth of about 100 WDM channels. For the computation, it was assumed that all three sections were 25 mm-long and that the differences in the grating period were applied in equal steps, that is to say, $\Lambda' = \Lambda - \Delta\Lambda/2$,

$\Lambda = \Lambda$, $\Lambda'' = \Lambda + \Delta\Lambda/2$. The grating period Λ that allowed maximum coupling for the fifth cladding mode at 1.55 μm was determined to be 399 μm, and the values of 2π and 6π were assumed, somewhat arbitrarily, for ϕ_1 and ϕ_2, respectively. The shaded area, marked "VALID REGION," corresponds to the region in which both constraints are satisfied and thus application of the TMCM is valid. The figure clearly shows the tradeoff relationship between the bandwidth and the maximum variation allowed in grating period, which was alluded to earlier. For example, $\Delta\Lambda$ is about 11 μm for $\Delta\lambda$ of 10 nm, whereas it is only about 6 μm when $\Delta\lambda$ is increased to 50 nm. Apparently, the TMCM does not allow a large margin for variation in the grating period, less than 5 %, in this particular example.

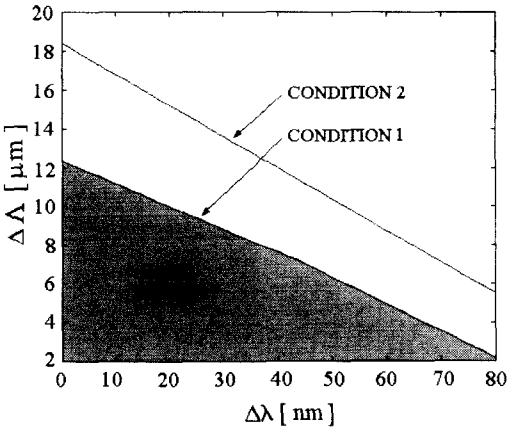

그림 4. 특정한 3-섹션 장주기 광섬유격자에서의 최대 허용 격자주기 변화 $\Delta\Lambda$와 대역폭 $\Delta\lambda$ 간의 관계

Fig. 4. Relationship between the maximum allowable variation in the grating period ($\Delta\Lambda$) and the bandwidth ($\Delta\lambda$) for a three-section LPFG.

As a side note, although related numerical results are not included here, one may easily determine, if so desired, how a change in the section lengths would affect the maximum allowable $\Delta\Lambda$ by noting that the results leading up to $\Delta\Lambda$ depend on ϕ_1/L and ϕ_2/L (see Eqs. (5) and (6), for example).

In summarizing this section, we conclude that based on the numerical results presented here there are definite constraints on the maximum allowable grating period variations in a cascaded LPFG, which become more severe with increasing bandwidth. These constraints should be carefully considered in designing or analyzing a multisection LPFG with the grating period as a design parameter, and should these constraints be violated, a multmode analysis must be carried out (see [4] for example).

Ⅳ. Conclusion

We examined the validity of the TMCM in the context of analyzing a cascaded LPFG consisting of multiple sections with different grating periods. A set of approximate conditions were proposed which would assure the validity of the TMCM's application to such a structure. Numerical examples demonstrate that these conditions impose a tradeoff between the maximum allowable grating period variation and the operating bandwidth for a multisection LPFG, for example a maximum fractional variation of the grating period of, say 4 %, for the bandwidth of $\Delta\lambda$ = 10 nm, which in turn may degrade the overall spectral characteristics of the cascade LPFG. These guidelines could serve as a valuable reference in design and analysis of cascaded LPFGs.

References

[1] G. Nykolak et al., "Impact of fiber grating on WDM system performance," *Proc. of OFC '98*, paper TuA3, 1998.

[2] A. M. Vensarkar, P. J. Lemaire, J. B. Judkins, V. Bhatia, T. Erdogan, and J. E. Sipe, "Long-period fiber gratings as band-rejection filters," *J. of Lightwave*

Technol., vol. 14, no. 1, pp. 58-64, 1996.

[3] T. Erdogan, "Cladding-mode resonances in short- and long-period fiber grating filters," *J. of Opt. Soc. of Am. A.*, vol. 14, no. 8, pp. 1760-1773, 1997.

[4] Y. Jeong and B. Lee, "Long-period fiber grating analysis using generalized N×N coupled-mode theory by section-wise discretization," *J. of Opt. Soc. of Kor.*, vol. 3, no. 2, pp. 55-63, 1999.

[5] H. Ke, K. S. Chiang, and J. H. Peng, "Analysis of phase-shifted long-period fiber gratings," *Photon. Technol. Lett.*, vol. 10, no. 11, pp. 1596-1598, 1998.

[6] H. Ghafouri-Shiraz and B. S. K. Lo, *Distributed feedback laser diode: principles and physical modeling*, Ch. 4, John Wiley & Sons, 1996.

저 자 소 개

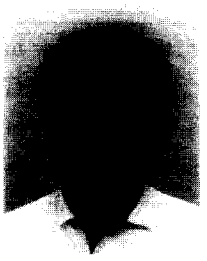

朴 東 旭(正會員)

1982, 1984, 1988년 미국 M.I.T. 전자전기컴퓨터공학부(EECS)에서 학사, 석사, 박사학위 취득. 1988~1990년 미국 플로리다 United Technologies Optical Systems의 레이저 레이다 그룹에서 연구원으로 CO_2 도파관 레이저와 레이저 레이다 응용에 관한 연구 수행. 1990~1991년 삼성전자(기흥)에서 선임연구원으로 마이크로파 레이다 시스템 개발. 1991년~현재 홍익대학교 전자공학과 부교수. 주 관심 연구분야는 광전자 (특히 DFB 반도체 레이저와 광섬유 격자 소자)와 마이크로파 및 레이저 레이다의 응용

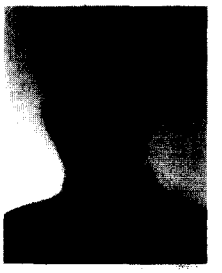

黃 俊 皖(學生會員)

1997, 1999년 홍익대학교 전자공학과 학사, 석사학위 취득. 1999년~현재 홍익대학교 전자공학과 박사과정. 2000년~현재 한국과학기술연구원 광기술연구센터 산학연구 프로그램 참여 중. 주관심 연구분야는 광섬유 격자 소자의 제작, 응용 및 해석